these observations is the direct interaction term, sometimes written in the form[3]:

$$\frac{d\sigma}{d\Omega} \propto 1-\frac{\mu^2 g^2 \sin^2\theta}{2k^4(1-\beta\cos\theta)^2}.$$

In positive meson photoproduction from hydrogen, this gives a forward maximum for the pions. If the photodisintegration cross section may be viewed as coming in part from the pickup of the forward pion by the remaining neutron in the deuteron, then this term in photoproduction would give a forward maximum to the observed proton angular distribution. Conversely, the same effect for negative pion production would tend to give a backward maximum for the protons in the photodisintegration process. The angular distribution in the forward direction, experimentally, is indeed observed to remain relatively high—although no detailed structure could be inferred from the existing data. In the backwards direction, however, the effect is significantly more pronounced, presumably because the other contributing terms are relatively small.

The principal result of this experiment is then to adduce additional evidence for the direct interaction term in meson photoproduction as exhibited in the photodisintegration process.

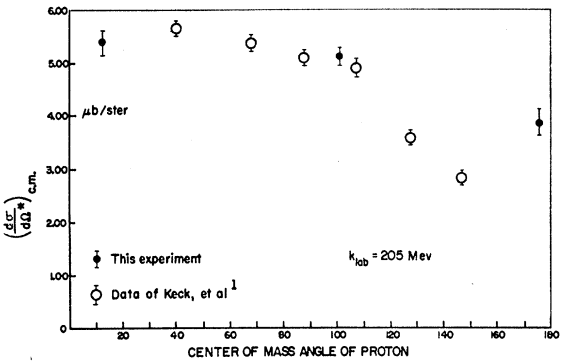

FIG. 6. Comparison of angular distributions for a photon energy of 205 Mev.

ACKNOWLEDGMENTS

The assistance of Mr. R. B. Engle, Mr. F. W. Markley, Mr. R. Fessel, and Mr. E. D. Metcalf of the synchrotron staff is gratefully acknowledged. We also wish to thank Professor P. H. Keesom and the low-temperature laboratory staff for furnishing the liquid hydrogen.

[3] M. Moravcsik, Phys. Rev. **104**, 1451 (1956). The notation here is that of this reference.

PHYSICAL REVIEW VOLUME 112, NUMBER 3 NOVEMBER 1, 1958

Radio-Frequency Orientation of Sb^{122}†*

FRANCIS M. PIPKIN
Lyman Laboratory, Harvard University, Cambridge, Massachusetts

(Received June 16, 1958)

Radioactive Sb^{122} donors in a doped silicon crystal have been oriented by saturation of forbidden transitions and by the Overhauser method. Double-resonance experiments in which an electron and a nuclear transition were saturated simultaneously were used to determine the Sb^{122} hyperfine splitting. A short discussion is given of how the nuclear relaxation mechanisms affect the double-resonance orientation signals. The hyperfine splitting of Sb^{122} has been found to be -132.59 ± 0.10 Mc/sec and its spin 2. The gyromagnetic ratio is -0.952 ± 0.010.

INTRODUCTION

THE technique of radio-frequency orientation[1–5] has been used to align the 65-hour Sb^{122} donors in an antimony-doped silicon crystal. Experiments similar[6] to those on As^{76} were performed in which the resultant anisotropy of the gamma rays emitted by the oriented nucleus was used to detect the nuclear resonance and hence to measure the nuclear hyperfine splitting of the radioactive isotope. The Sb^{122} forms an instructive contrast to As^{76} in that the relaxation time for the nuclear orientation is much shorter for the antimony donors than for the arsenic donors.[7] The fact that part of this nuclear relaxation is due to processes in which the nucleus and electron change their state simultaneously is demonstrated by successful experiments in which orientation was produced by the Overhauser method.

The shorter nuclear relaxation time for the Sb^{122}

† This research was supported in part by the Physics Department, Harvard University, and a grant from the National Science Foundation.

* A preliminary account of this work has been given [F. M. Pipkin, Bull. Am. Phys. Soc. Ser. II, 3, 8 (1958)].

[1] A. Kastler, Compt. rend. **233**, 1444 (1954).
[2] A. W. Overhauser, Phys. Rev. **92**, 411 (1953).
[3] A. Abragam, Phys. Rev. **98**, 1728 (1955).
[4] G. Feher, Phys. Rev. **103**, 500 (1956).
[5] C. D. Jeffries, Phys. Rev. **106**, 164 (1957).
[6] F. M. Pipkin and J. W. Culvahouse, Phys. Rev. **109**, 1423 (1958).
[7] J. W. Culvahouse and F. M. Pipkin, Phys. Rev. **109**, 319 (1958).

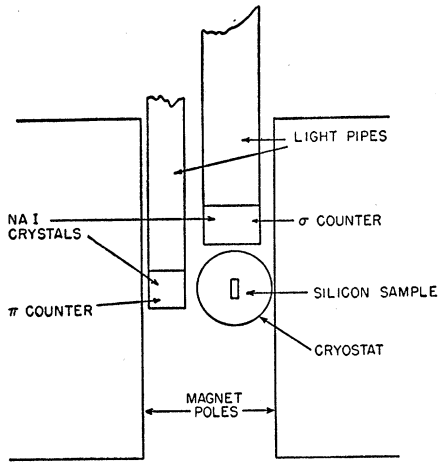

FIG. 1. Diagram showing the relative positions of the two counters with respect to the sample.

donors made it difficult to use an experiment in which the orientation was first produced by the saturation of a $\Delta(m_I+m_J)=0$ forbidden transition and subsequently destroyed by the application of another radio-frequency field to measure the frequency of the direct nuclear transitions. Instead a double-resonance experiment was performed; one of the electron transitions was saturated while the low-frequency oscillator was swept over the region of the nuclear transitions. When certain of the nuclear transitions were saturated, there was a modulation of the Overhauser orientation.

In order to understand the structure of the orientation signals it seems necessary to invoke other relaxation processes than the direct electron relaxation and the cross relaxation in which the electron and the nucleus change their state simultaneously so that the component of the total angular momentum along the axis of quantization remains constant. The signals can be understood qualitatively through the introduction of the quadrupole relaxation or of a general tensor interaction between the electron spin and the nuclear spin such as would be produced by a time-dependent anisotropic hyperfine interaction.[3] No detailed calculations of the effect of these additional relaxation mechanisms upon the dynamics of the orientation have been made; instead attention has been focused upon how they influence the equilibrium populations. Only enough of the theory is included in this paper to permit an understanding of the measurement of the nuclear magnetic moment of Sb^{122}. For additional information on the method of dynamic nuclear orientation other sources should be consulted.[6,8]

APPARATUS

Most of the apparatus used in this experiment has been described in the paper[6] on As[76]. The only major modification was an enlargement of the magnet gap from 3 in. to 3.5 in. so that the number of gamma rays emitted in the direction of (π position) and perpendicular to (σ position) the magnetic field could be observed simultaneously. The physical arrangement of the counters is shown in Fig. 1. The π counter consists of a 1-in. by 1-in. NaI(Tl) crystal which is coupled by a 13-in. long, 1-in. o.d. Lucite light pipe to an RCA-6199 photomultiplier. No stabilization is provided for the π counter; it is considerably more unstable than the σ counter.

The antimony-doped silicon samples used in this experiment were obtained from the Bell Telephone Laboratories. They were cut into rectangular pieces 0.170-in. by 0.420 in. by 0.485 in. and etched with CP-4 until they fitted inside the rectangular waveguide cavities. The nominal doping was 4×10^{16} donors per cm^3. The crystals were irradiated in the Materials Testing Reactor at Arco, Idaho, for 24 hours in a flux of 10^{14} thermal neutrons/cm^2 sec. The samples were subsequently annealed in vacuum for 4 to 6 hours at a temperature of 1100°C.

REVIEW OF THE THEORY

A. Description of Nuclear Orientation

The decay scheme of 65-hour Sb^{122} has been extensively investigated by many workers, among whom the principal ones are Glaubman[9] and Farrelly *et al.*[10] The results of these studies are summarized in Fig. 2. The unique first-forbidden shape of the 1.987-Mev beta ray leads to the assignment of spin 2 and negative parity to the ground state of Sb^{122}. This is also confirmed by the comparison of the experimental and theoretical K capture-positron ratios for the $Sb^{122}\rightarrow Sn^{122}$ ground-state transition.[11] The 1.423-Mev beta ray is a first-forbidden transition with an allowed shape which displays beta-gamma angular correlation.[12] The existence of the angular correlation is attributed to an interference between the components of the decay which carry off angular momenta 0, 1, and 2. The spin and parity assignments for the excited states of Te^{122} have been made from a study of the beta-gamma and gamma-gamma angular correlations.[13] The radiations γ_1 and γ_3 are pure electric quadrupole; the radiation γ_2 is a mixture of $(92\pm4)\%$ electric quadrupole and $(8\pm4)\%$ magnetic dipole. The mean life of the 563-kev state of Te^{122} has been found to be 1.5×10^{-10} sec by coincidence techniques[14] and 1.4×10^{-11} sec by a study of the Coulomb excitation[15] of the 563-kev level.

[8] M. J. Steinland and H. A. Tolhoek, in *Progress in Low-Temperature Physics*, edited by C. J. Gorter (North-Holland Publishing Company, Amsterdam, 1957), Chap. 10, p. 292.

[9] M. J. Glaubman, Phys. Rev. **98**, 645 (1955).
[10] Farrelly, Koerts, Benczer, Van Lieshout, and Wu, Phys. Rev. **99**, 1440 (1955).
[11] Perlman, Welker, and Wolfsberg, Phys. Rev. **110**, 381 (1958).
[12] I. Shaknov, Phys. Rev. **82**, 333(A) (1951).
[13] F. Lindqvist and I. Marklund, Nuclear Phys. **4**, 189 (1957).
[14] C. F. Coleman, Phil. Mag. **46**, 1135 (1955).
[15] G. M. Temmer and N. P. Heydenburg, Phys. Rev. **104**, 967 (1956).

In this orientation experiment the gamma rays are observed. An examination of the relative intensities of the gamma rays shown in Fig. 2 shows that 93% of them are due to γ_1. For the interpretation of the experiments in this paper it will be assumed that the other gamma rays can be ignored. If j_0 denotes the spin of the ground state of Sb^{122} and the a_{m_0} are the populations of its nuclear substates normalized so that their sum is one, then the excess of the number of the quadrupole gamma rays, γ_1, emitted at an angle θ with respect to the magnetic field, over the number emitted with random nuclear orientation, expressed as a fraction of the number emitted with random nuclear orientation, is given by[16]

$$S(\theta)=-(10/7)f_2B_2P_2(\cos\theta)-(40/3)f_4B_4P_4(\cos\theta), \quad (1)$$

where

$$f_2=\frac{1}{j_0^2}\left[\sum_{m_0} m_0^2 a_{m_0}-\tfrac{1}{3}j_0(j_0+1)\right], \quad (2)$$

$$f_4=\frac{1}{j_0^4}\left[\sum_{m_0} m_0^4 a_{m_0}-(1/7)(6j_0^2+6j_0-5)\sum_{m_0} a_{m_0}m_0^2 +(3/35)j_0(j_0-1)(j_0+1)(j_0+2)\right], \quad (3)$$

and the spherical harmonics are given by

$$P_2(\cos\theta)=\tfrac{3}{2}(\cos^2\theta-\tfrac{1}{3}), \quad (4)$$

$$P_4(\cos\theta)=(35/8)[\cos^4\theta-(6/7)\cos^2\theta+(3/35)]. \quad (5)$$

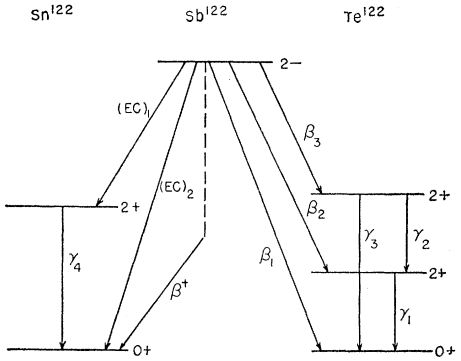

RADIATION	ENERGY	INTENSITY	LOG ft
β_1	1.987	26.5 %	8.6
β_2	1.423	69.0 %	7.6
β_3	0.730	4.4 %	7.7
β^+	~ 0.44	0.005 %	—
$(EC)_1$	0.3	0.8 %	—
$(EC)_2$	1.45	2.2 %	—
γ_1	0.563	73.0 %	EQ
γ_2	0.693	3.6 %	EQ+MD
γ_3	1.256	0.8 %	EQ
γ_4	1.152	0.8 %	—

FIG. 2. Nuclear energy level diagram for Sb^{122}.

[16] S. R. DeGroot and H. A. Tolhoek, in *Beta- and Gamma-Ray Spectroscopy*, edited by K. Siegbahn (North-Holland Publishing Company, Amsterdam, 1955), Chap. 19, Part III, p. 613.

The parameters B_2 and B_4 are attenuation factors which depend upon the character of the first forbidden transition β_2. If α_0, α_1, and α_2 represent the relative probabilities that the beta ray[17] carries off angular momenta, 0, 1, and 2, respectively, normalized so that their sum is unity, then

$$B_2=1-\alpha_1/2-17\alpha_2/14, \quad (6)$$

$$B_4=1-5\alpha_1/3-5\alpha_2/7. \quad (7)$$

The signals $S(\sigma)$ and $S(\pi)$ which are defined as the fractional changes in counting rate for observation perpendicular to and along the direction of the magnetic field, respectively, are given by

$$S(\sigma)=5B_2f_2/7-5B_4f_4, \quad (8)$$

$$S(\pi)=-10B_2f_2/7-40B_4f_4/3. \quad (9)$$

In this experiment no attempt has been made to determine α_0, α_1, and α_2; for sample calculations to illustrate the effect of the relaxation mechanisms upon the signals it will be assumed that β_2 carries away no angular momentum.

B. Description of the Donor Atom

The Hamiltonian for an antimony donor atom in its $^2S_{\frac{1}{2}}$ electronic ground state in an external magnetic field H is

$$\mathcal{H}=-g_J\mu_0(\mathbf{J}\cdot\mathbf{H})-g_I\mu_n(\mathbf{I}\cdot\mathbf{H})+A(\mathbf{I}\cdot\mathbf{J}), \quad (10)$$

where g_J is gyromagnetic ratio of the electron, g_I is the gyromagnetic ratio of the antimony nucleus, A the hyperfine interaction constant, μ_0 the Bohr magneton, and μ_n the nuclear magneton. A convention has been adopted in which the electron gyromagnetic ratio is negative and A is positive for a positive nuclear moment. If the magnetic sublevels of the donor atom are designated by the number pairs (m_J,m_I), then to second order in the hyperfine interaction their energies are

$$E_{m_J,m_I}=-g_J\mu_0Hm_J-g_I\mu_nHm_I+Am_Im_J +(A^2/4\mu_0H)m_J(I-2m_Jm_I)(I+2m_Jm_I+1). \quad (11)$$

Figure 3 shows the energy levels for nuclear spin 2 and a negative nuclear magnetic moment.

If $P(m_J,m_I)$ are the occupation probabilities of the various substates of the donor atom normalized so that their sum is one and the $W(m_J,m_I|m_J',m_I')$ are the factors common to the $(\frac{1}{2},m_I)\rightarrow(-\frac{1}{2},m_I')$ and the $(-\frac{1}{2},m_I')\rightarrow(\frac{1}{2},m_I)$ transition probabilities, then the change in time of the level populations can be described

[17] E. Konopinski, in *Beta- and Gamma-Ray Spectroscopy*, edited by K. Siegbahn (North-Holland Publishing Company, Amsterdam, 1955), Chap. 10, p. 292.

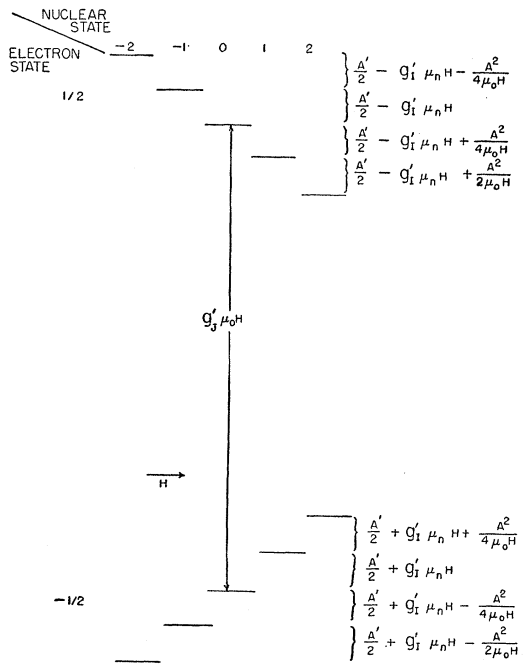

FIG. 3. Energy levels for donor atom with nuclear spin 2 and a negative nuclear magnetic moment in a large magnetic field. The arrow with the H indicates the order in which the lines are displayed as a function of magnetic field with a fixed oscillator frequency. The primes in the figure denote absolute values.

by the set of equations

$$\dot{P}(m_J,m_I)=\sum_{m_I',m_J'} W(m_J,m_I|m_J',m_I') \times[e^{-(\mu_0H/kT)(m_J-m_J')}P(m_J',m_I') - e^{-(\mu_0H/kT)(m_J'-m_J)}P(m_J,m_I)]. \quad (12)$$

For the calculation of the Boltzmann factors, the hyperfine contribution to the energy has been neglected. For this experiment, interest is centered on the equilibrium configuration of the level populations when one of the electron transitions is being saturated. In this case in addition to the relaxation processes there is a saturating radio-frequency field; it essentially cancels the effect of the Boltzmann factor for one of the electron transitions.

For the antimony donors the following three mechanisms would be expected to furnish the principal means of nuclear relaxation. For an atomic spin of $\frac{1}{2}$ they can be conveniently expressed in terms of the Clebsch-Gordan coefficients.

(1) The cross relaxation produced by modulation of the isotropic hyperfine interaction,

$$W(m_J,m_I|m_J',m_I')=\omega_1(I1m_I'\mu|I1Im_I)^2 \times(1-\delta m_J,m_J')\delta m_I+m_J,m_I'+m_J'; \quad (13)$$

(2) nuclear quadrupole relaxation,

$$W(m_J,m_I|m_J',m_I')=\omega_3(I2m_I'\mu|I2Im_I)^2\delta m_J',m_J; \quad (14)$$

(3) nuclear relaxation produced by the modulation of an anisotropic hyperfine interaction of the form

$$\sum_{\alpha,\beta=1}^{3} A_{\alpha\beta}I_\alpha J_\beta. \quad (15)$$

Here $A_{\alpha\beta}$ is a symmetric tensor and I_α and J_β are components of the angular momentum operators for the nucleus and the electron, respectively. If Eq. (15) is decomposed in terms of Clebsch-Gordan coefficients into process yielding nuclear relaxation, it becomes

$$(I1m_I'\mu|I1Im_I)^2\{(1-\delta m_J,m_J') [\omega_3\delta m_J-m_J',m_I-m_I'+\omega_4\delta m_J+m_I,m_J'+m_I'] +\omega_5\delta m_J,m_J'(1-\delta m_I,m_I')\}. \quad (16)$$

The ω_4 contribution of the anisotropic hyperfine interaction can be regarded as an addition to the relaxation from the isotropic hyperfine interaction. Relaxation mechanisms with a factor $(1-\delta m_J,m_J')$ can produce orientation when one of the electron transitions is saturated; those with $\delta m_J,m_J'$ cannot.

For the Sb^{122} donors the nuclear relaxation time is much longer than the direct electron relaxation time; consequently, it is advantageous to introduce the new variables

$$P^+(m)=P(-\tfrac{1}{2},m_I)+P(\tfrac{1}{2},m_I), \quad (17)$$

$$P^-(m)=\alpha P(-\tfrac{1}{2},m_I)-P(\tfrac{1}{2},m_I), \quad (18)$$

where

$$\alpha=e^{-(2\mu_0H/kT)}, \quad (19)$$

and m now refers to the nuclear substate. If it is then assumed that

$$P^-(m)=0 \quad (20)$$

the general relaxation equation, Eq. (12), reduces to the form

$$\dot{P}^+(m)=\textstyle\sum_{m'} W(m|m')[P^+(m')-P^+(m)]. \quad (21)$$

The $W(m|m')$ will be called the reduced relaxation matrix. For the three nuclear relaxation mechanisms which have been considered, the reduced W's are

(1) isotropic hyperfine relaxation,

$$W(m|m')=[\alpha^{\frac{1}{2}}/(1+\alpha)]\omega_1(I1m'\mu|I1Im)^2 \times(1-\delta m,m'); \quad (22)$$

(2) nuclear quadrupole relaxation,

$$W(m|m')=\omega_2(I2m'\mu|I2Im)^2(1-\delta m,m'); \quad (23)$$

(3) anisotropic hyperfine relaxation,

$$W(m|m')=[(\omega_3+\omega_4)\alpha^{\frac{1}{2}}/(1+\alpha)+\omega_5] \times(I1m'\mu|I1Im)^2(1-\delta m,m'). \quad (24)$$

In terms of the Clebsch-Gordan coefficients there are only two types of relaxation-dipole and quadrupole. For situations where the reduced equations can be used, the change of the f_2 and f_4 parameters due to the

nuclear relaxation can be described by the equations,[7]

$$f_2(t)=f_2(0)e^{-\lambda_2 t}, \tag{25}$$

$$f_4(t)=f_4(0)e^{-\lambda_4 t}, \tag{26}$$

where

$$\lambda_2=\tfrac{1}{2}\{[\alpha^{\frac{1}{2}}/(1+\alpha)](\omega_1+\omega_2+\omega_4)+\omega_5\}+(5/7)\omega_2, \tag{27}$$

$$\lambda_4=(5/3)\{[\alpha^{\frac{1}{2}}/(1+\alpha)](\omega_1+\omega_2+\omega_4)+\omega_5\}+(17/14)\omega_2. \tag{28}$$

For situations where a radio-frequency field is being applied to saturate the $(\frac{1}{2},m_R)\rightarrow(-\frac{1}{2},m_R)$ electron transition, the auxiliary variables

$$\begin{aligned}P^+(m)&=P(-\tfrac{1}{2},m_I)+P(\tfrac{1}{2},m_I),\\ P^-(m)&=\alpha P(-\tfrac{1}{2},m_I)-P(\tfrac{1}{2},m_I),\end{aligned} \tag{29}$$

can be introduced for $m\neq m_R$, and for $m=m_R$ the set

$$\begin{aligned}P^+(m_R)&=P(-\tfrac{1}{2},m_R)+P(\tfrac{1}{2},m_R),\\ P^-(m_R)&=P(-\tfrac{1}{2},m_R)-P(\tfrac{1}{2},m_R).\end{aligned} \tag{30}$$

This makes it possible to obtain a reduced set of equations in which the effect of the saturation is automatically taken into account. In this experiment only situations where the central $(-\frac{1}{2},0)\rightarrow(\frac{1}{2},0)$ transition is saturated are important. For this case the time dependence of the nuclear populations is given by the following equations:

(a) For cross relaxations of the form

$$\Delta(m_I+m_J)=0 \quad (\omega_1 \text{ and } \omega_4), \tag{31}$$

one has

$$\begin{bmatrix}\dot P_{-2}\\ \dot P_{-1}\\ \dot P_0\\ \dot P_1\\ \dot P_2\end{bmatrix}=\frac{\alpha^{\frac{1}{2}}(\omega_1+\omega_4)}{12(1+\alpha)}\begin{bmatrix}-4 & 4 & 0 & 0 & 0\\ 4 & -10 & 3(1+\alpha) & 0 & 0\\ 0 & 6 & -3(1+\alpha)^2/\alpha & 6 & 0\\ 0 & 0 & 3(1+\alpha)/\alpha & -10 & 4\\ 0 & 0 & 0 & 4 & -4\end{bmatrix}\begin{bmatrix}P_{-2}\\ P_{-1}\\ P_0\\ P_1\\ P_2\end{bmatrix}. \tag{32}$$

(b) For cross relaxations of the form $\Delta(m_I+m_J)=\pm 2$, one has

$$\begin{bmatrix}\dot P_{-2}\\ \dot P_{-1}\\ \dot P_0\\ \dot P_1\\ \dot P_2\end{bmatrix}=\frac{\alpha^{\frac{1}{2}}\omega_3}{12(1+\alpha)}\begin{bmatrix}-4 & 4 & 0 & 0 & 0\\ 4 & -10 & 3(1+\alpha)/\alpha & 0 & 0\\ 0 & 6 & -3(1+\alpha)^2/\alpha & 6 & 0\\ 0 & 0 & 3(1+\alpha) & -10 & 4\\ 0 & 0 & 0 & 4 & -4\end{bmatrix}\begin{bmatrix}P_{-2}\\ P_{-1}\\ P_0\\ P_1\\ P_2\end{bmatrix}.$$

There is no change in the equations for the other mechanisms (ω_2 and ω_5).

C. Expected Form for the Orientation Signals

In order to understand the experiments on the measurement of the spin and nuclear magnetic moment of the radioactive antimony, the manner in which the nuclear relaxation mechanisms affect the signals must be known. No detailed calculations have been made to determine the exact behavior of the nuclear populations as a function of time. Instead, interest has been focused on the general features of the development in time of the orientation signals and on the way the relaxation mechanisms influence the signals for double-resonance experiments.

Unless the nuclear relaxation time is very short, orientation can always be produced by the saturation of the forbidden $\Delta(m_I+m_J)=0$ transitions. Figure 4 shows the expected form of the signals when a radio-frequency field is applied so as to saturate the forbidden transitions and the nuclear relaxation time is such that the orientation decays during the time spent in moving the magnetic field between adjacent transitions. That these are forbidden transitions can be ascertained by observing the manner in which the orientation develops after the saturation is started. Figure 5(a) shows the expected behavior for a forbidden transition. There is an initial fast rise followed by a slow increase determined by the relaxation time for $(-\frac{1}{2},m)\rightarrow(\frac{1}{2},m)$ transitions.

The mechanism for the observed nuclear relaxation can be studied by experiments in which it is attempted to produce orientation through the Overhauser effect. If part of the nuclear relaxation is due to processes in which the nucleus and electron change states simultaneously, then it may be possible to produce orientation by the saturation of an electron transition. The development in time of the orientation signal for saturation of the $(-\frac{1}{2},0)\rightarrow(\frac{1}{2},0)$ transition is shown in Fig. 5(b). The magnitude of the signal depends upon the mechanisms producing the nuclear relaxation; the

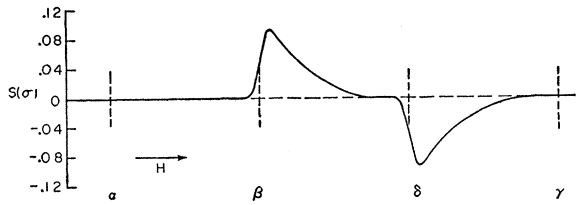

FIG. 4. Expected σ-position signals for saturation of the forbidden transitions. For a negative nuclear magnetic moment α is the $(\frac{1}{2},-2)\rightarrow(-\frac{1}{2},-1)$ transition, β the $(\frac{1}{2},-1)\rightarrow(-\frac{1}{2},0)$ transition, δ the $(\frac{1}{2},0)\rightarrow(-\frac{1}{2},1)$ transition, and γ the $(\frac{1}{2},1)\rightarrow(-\frac{1}{2},2)$ transition. The signals have been computed assuming no angular momentum is carried off by the beta ray and electric quadrupole nuclear relaxation.

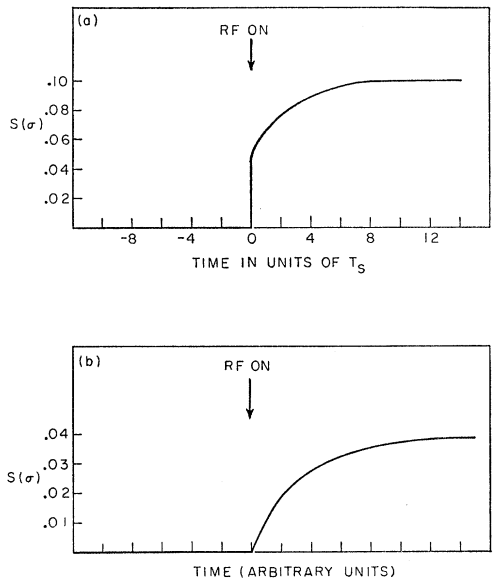

FIG. 5. (a) The growth in time for the σ-position signal for saturation of the $(\frac{1}{2}, -1)\rightarrow(-\frac{1}{2}, 0)$ forbidden transition. The signal has been computed assuming no angular momentum is carried off by the beta ray. T_s is the relaxation time for the $(\frac{1}{2},m)\rightarrow(-\frac{1}{2}, m)$ electron transitions. (b) The growth in time of the σ-position Overhauser signal for saturation of the $(\frac{1}{2},0)\rightarrow(-\frac{1}{2}, 0)$ electron transition. It has been assumed that all nuclear relaxation is due to the isotropic hyperfine interaction.

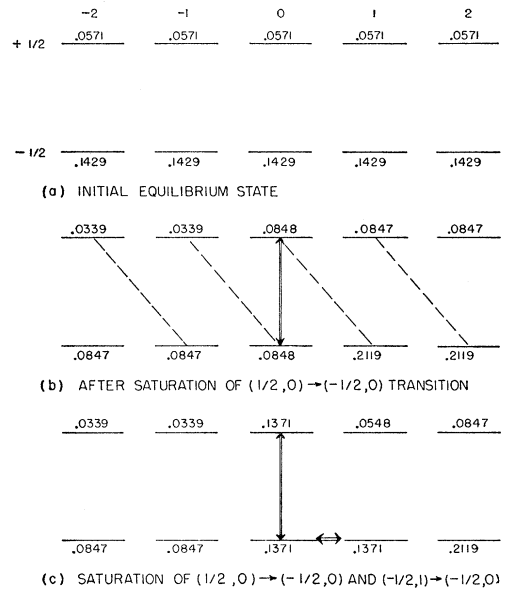

FIG. 6. Schematic representation of the calculation of the nuclear populations for the double-resonance experiments. The calculations were made for $T=1.25°K$ and $H=8500$ gauss. It has been assumed that there is no nuclear relaxation while the nuclear transition is being saturated. This particular calculation is for relaxation due only to the isotropic hyperfine interaction.

rise time of the signal depends upon the relaxation time for processes which produce the orientation; the fall time depends upon all the nuclear relaxation mechanisms.

The most sensitive test for the presence of relaxation mechanisms other than the isotropic hyperfine interaction is the structure of the double-resonance signals. The double-resonance experiments are performed by first applying a radio-frequency field to saturate the $(-\frac{1}{2}, 0)\rightarrow(\frac{1}{2},0)$ transition. When a new equilibrium has been established, another oscillator is swept over the region of the $(-\frac{1}{2}, m)\rightarrow(-\frac{1}{2}, m\pm1)$ nuclear transitions. For a negative nuclear magnetic moment, when sweeping from low to high frequency, the first transition to be observed is the $(-\frac{1}{2}, -1)\rightarrow(-\frac{1}{2}, 0)$ transition; when sweeping from high to low, it will be the $(-\frac{1}{2}, 1)\rightarrow(-\frac{1}{2}, 0)$ transition. The ratio of the amplitude of these two signals is a sensitive function of the dilution of the isotropic hyperfine relaxation with other relaxation mechanisms.

In Table I are summarized the equilibrium populations of the nuclear sublevels for various mixtures of the nuclear quadrupole relaxation with isotropic hyperfine relaxation. Also the σ position signals have been calculated for the equilibrium Overhauser saturation and the two double-resonance experiments. The method of calculation for the double-resonance signals is illustrated in Fig. 6. Figure 7 gives a graphic representation of the expected double-resonance signals for a mixture of quadrupole and hyperfine relaxation when the low-frequency oscillator is swept up through the $(-\frac{1}{2}, m)\rightarrow(-\frac{1}{2}, m+1)$ nuclear transitions. Here the idealization has been made that the frequency separation of the nuclear transitions is much greater than their line width.

TABLE I. Nuclear populations and alignment signals expected for Overhauser effect and double-resonance experiments. The relaxation is assumed to be due to a mixture of the isotropic hyperfine (ω_1) and the nuclear quadrupole (ω_2) mechanisms. It has been assumed that the beta ray carries away no angular momentum. $S_0(\sigma)$ is the Overhauser signal for saturation of the $(-\frac{1}{2}, 0)\rightarrow(\frac{1}{2},0)$ transition; $S_{-1}(\sigma)$ is the signal for simultaneous saturation of the $(-\frac{1}{2}, 0)\rightarrow(\frac{1}{2},0)$ and the $(-\frac{1}{2}, -1)\rightarrow(-\frac{1}{2}, 0)$ transitions; $S_{+1}(\sigma)$ is the signal for simultaneous saturation of the $(-\frac{1}{2}, 0)\rightarrow(\frac{1}{2},0)$ and the $(-\frac{1}{2}, 1)\rightarrow(-\frac{1}{2}, 0)$ transitions.

Relaxation mixture ω_2/ω_1	Nuclear populations for Overhauser saturation					Signals in σ position		
	a_{-2}	a_{-1}	a_0	a_1	a_2	$S_0(\sigma)$	$S_{-1}(\sigma)$	$S_{+1}(\sigma)$
0	0.1186	0.1186	0.1695	0.2966	0.2966	+0.0381	+0.0381	−0.0928
0.158	0.1610	0.1578	0.1762	0.2597	0.2454	+0.0298	+0.0045	−0.0705
0.316	0.1741	0.1723	0.1797	0.2448	0.2292	+0.0254	−0.0088	−0.0623
0.527	0.1819	0.1815	0.1828	0.2342	0.2195	+0.0215	−0.0178	−0.0565
1.581	0.1925	0.1941	0.1896	0.2167	0.2072	+0.0130	−0.0323	−0.0488
∞	0.2000	0.2000	0.2000	0.2000	0.2000	+0.0000	−0.0440	−0.0440

TABLE II. Nuclear populations and alignment signals expected for Overhauser effect and double resonance experiments. The relaxation is assumed to be due to a mixture of the isotropic hyperfine (ω_1) and the anisotropic hyperfine (ω_3 and ω_4) mechanisms. It has been assumed that the beta ray carries away no angular momentum. $S_0(\sigma)$ is the Overhauser signal for saturation of the $(-\frac{1}{2}, 0)\rightarrow(\frac{1}{2},0)$ transition; $S_{-1}(\sigma)$ is the signal for simultaneous saturation of the $(-\frac{1}{2}, 0)\rightarrow(\frac{1}{2},0)$ and the $(-\frac{1}{2}, -1)\rightarrow(-\frac{1}{2}, 0)$ transitions; $S_{+1}(\sigma)$ is the signal for simultaneous saturation of the $(-\frac{1}{2}, 0)\rightarrow(\frac{1}{2},0)$ and the $(-\frac{1}{2}, 1)\rightarrow(\frac{1}{2},0)$ transitions.

Relaxation mixture $\omega_3/(\omega_1+\omega_4)$	Nuclear populations for Overhauser saturation					Signals in σ position		
	a_{-2}	a_{-1}	a_0	a_1	a_2	$S_0(\sigma)$	$S_{-1}(\sigma)$	$S_1(\sigma)$
0	0.1186	0.1186	0.1694	0.2965	0.2965	+0.0383	+0.0383	−0.0925
0.2	0.1483	0.1483	0.1695	0.2669	0.2669	+0.0383	+0.0164	−0.0710
0.4	0.1695	0.1695	0.1694	0.2458	0.2458	+0.0383	+0.0008	−0.0552
1.0	0.2076	0.2076	0.1694	0.2076	0.2076	+0.0383	−0.0273	−0.0273
2.0	0.2373	0.2373	0.1695	0.1780	0.1780	+0.0383	−0.0490	−0.0055
∞	0.2965	0.2965	0.1695	0.1186	0.1186	+0.0383	−0.0925	+0.0383

In Table II are summarized the results of a similar set of calculations for a mixture of the isotropic hyperfine interaction and the anisotropic hyperfine interaction. To simplify the calculation, the ω_5 part of the anisotropic interaction has been ignored.

RESULTS OF THE EXPERIMENT

A. Initial Orientation Experiments

The Sb^{122} was first oriented by the saturation of the $\Delta(m_I+m_J)=0$ forbidden transitions. The silicon sample was placed in a rectangular wave-guide cavity and the cavity was oriented so that there was a component of the radio-frequency magnetic field in the direction of the dc magnetic field. The dc magnetic field was then moved slowly through the region of the stable Sb^{121} resonances and the number of gamma rays emitted in the σ position observed. A plot of the observed counting rate *versus* magnetic field is shown in Fig. 8. Two signals are observed. A comparison with the expected signals shown in Fig. 4 indicates that these are the $(\frac{1}{2}, -1)\rightarrow(-\frac{1}{2}, 0)$ and the $(\frac{1}{2},0)\rightarrow(-\frac{1}{2}, 1)$ forbidden transitions and that the hyperfine splitting of the Sb^{122} is approximately 130 Mc/sec.

To confirm this assignment, two auxiliary experiments were performed. The radio-frequency power was turned off and the dc magnetic field was set at the value corresponding to the low-field transition of the two signals in Fig. 8. After the counting rate had been observed to establish a reference level, the radio-frequency field was turned on. A plot of the observed counting rate *versus* time is shown in Fig. 9(a). The fast rise and slow decay of the orientation is just what would be expected for the saturation of a forbidden transition where the nuclear relaxation time is several times longer than the electron relaxation time.

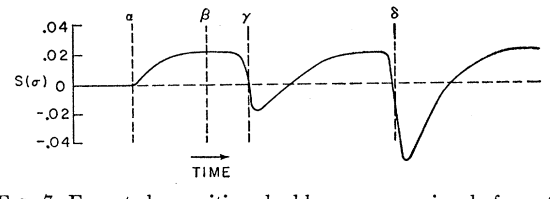

FIG. 7. Expected σ-position double-resonance signals for saturation of the $(\frac{1}{2},0)\rightarrow(-\frac{1}{2}, 0)$ electron transition and movement of the nuclear frequency up through the resonance values. This calculation is for the $\omega_2/\omega_1=0.527$ mixture of quadrupole and isotropic hyperfine relaxation. At α the saturation of the $(\frac{1}{2},0)\rightarrow(-\frac{1}{2}, 0)$ transition is begun; at β the low-frequency oscillator is turned on; at γ the nuclear transition $(-\frac{1}{2}, -1)\rightarrow(-\frac{1}{2}, 0)$ is saturated; at δ the $(-\frac{1}{2}, 0)\rightarrow(-\frac{1}{2}, 1)$ transition is saturated. It has been assumed that the beta ray carries away no angular momentum.

The radio-frequency field was then turned off again and the magnetic field set at a point midway between the observed positions of the forbidden transitions. This is where the $(-\frac{1}{2}, 0)\rightarrow(\frac{1}{2},0)$ transition would be expected. Again, a reference level for the counting rate was established and then the counting rate was observed after the radio-frequency field was turned on. In this case [Fig. 9(b)] the signal develops quite slowly with a time constant comparable to that for the relaxation of the orientation in Fig. 8. Thus it is concluded that this orientation is due to the Overhauser effect and that part of the nuclear relaxation is due to the modulation of the hyperfine interaction.

Since the Overhauser orientation always decreases the population of the $m=0$ nuclear substate and in this experiment increases the counting rate, it is concluded that the low-field forbidden transition decreases the population of the $m=0$ level and hence that the sign of the nuclear magnetic moment is negative.

B. Precise Measurement of the Hyperfine Splitting

In order to further confirm the conclusion that the two forbidden transitions were the pair $(-\frac{1}{2}, 0)\rightarrow(\frac{1}{2},1)$

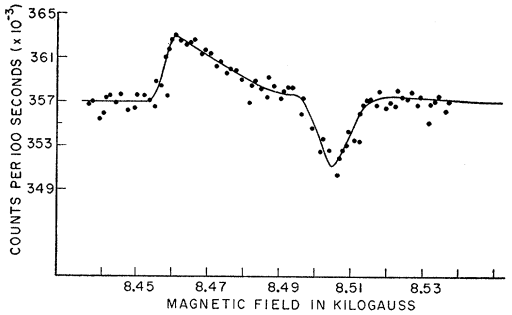

FIG. 8. Plot of σ-position counting rate *versus* magnetic field for saturation of the forbidden transitions. Movement is from low to high magnetic field. Each point represents observation for 100 sec.

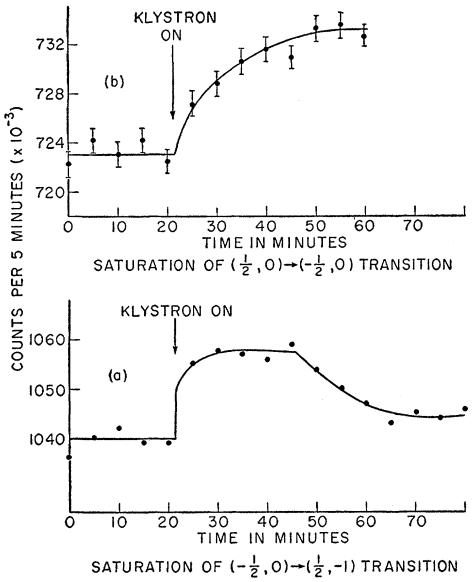

FIG. 9. (a) Plot of counting rate *versus* time for saturation of $(\frac{1}{2}, -1)\rightarrow(-\frac{1}{2}, 0)$ transition. Also part of the decay after the radio-frequency field is turned off is shown. (b) Plot of counting rate *versus* time (σ position) for saturation of $(-\frac{1}{2}, 0)\rightarrow(\frac{1}{2},0)$ transition.

and $(\frac{1}{2},0)\rightarrow(-\frac{1}{2}, 1)$ and to obtain a more precise value for the hyperfine splitting, a series of double-resonance experiments were performed. A radio-frequency field was first applied to saturate the $(-\frac{1}{2}, 0)\rightarrow(\frac{1}{2},0)$ electron transition. Then after an equilibrium value of the Overhauser orientation had been obtained and with the first radio-frequency field still on, a second radio-frequency field was swept over the region of 72 Mc/sec so as to saturate the $(-\frac{1}{2}, m)\rightarrow(-\frac{1}{2}, m\pm1)$ nuclear transitions. A plot of the counting rate *versus* time for such an experiment showing first the increase of the counting rate due to the Overhauser effect and then the decrease due to the saturation of the nuclear transitions is shown in Fig. 10. Whenever possible, runs

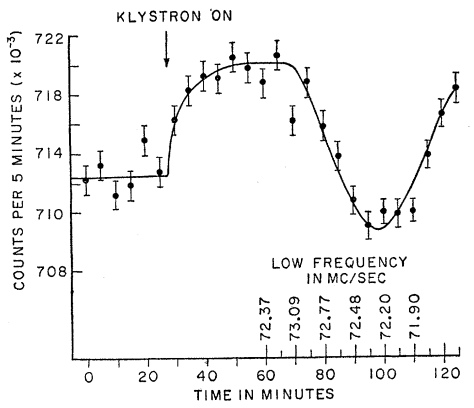

FIG. 10. Plot of counting rate in σ position *versus* time showing the formation of the Overhauser orientation and the subsequent decrease in counting rate when the nuclear transitions are saturated.

were made in pairs so that each time the magnetic field was set so that the $(\frac{1}{2},0)\rightarrow(-\frac{1}{2}, 0)$ transition was saturated, the nuclear transitions were observed both with increasing frequency and with decreasing frequency. A pair of such transitions is shown in Fig. 11. In Table III are summarized the results of all the double-resonance experiments. The frequency of a transition has been taken to be that frequency at which the change in counting rate is one-half of its maximum value.

Only one transition is observed going each direction in frequency and these two transitions are separated by approximately 600 kc/sec. The expected line width for the nuclear transitions is about 120 kc/sec and their separation 400 kc/sec. From this it is concluded that the observed transitions are $(-\frac{1}{2}, 1)\rightarrow(-\frac{1}{2}, 0)$ and $(-\frac{1}{2}, 0)\rightarrow(-\frac{1}{2}, -1)$. There are two ways in which the near equality in magnitude of these signals could be explained. When the radio-frequency field is applied to saturate the $(-\frac{1}{2}, 0)\rightarrow(\frac{1}{2},0)$ transition, the dc magnetic

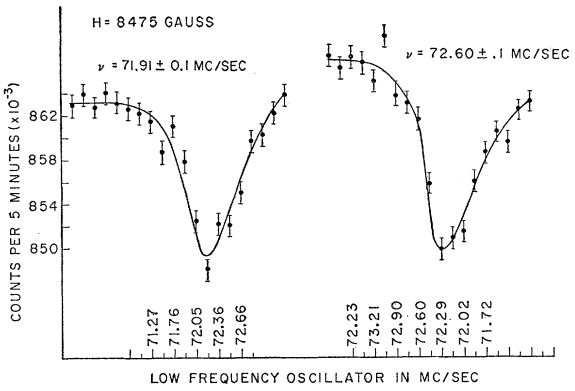

FIG. 11. Plot of σ-position counting rate *versus* frequency of the second radio-frequency field for moving both upwards and downwards in frequency.

field is sinusoidally modulated by approximately 10 gauss peak to peak so as to completely saturate the transition. If at the same time there were complete saturation of the $(\frac{1}{2}, -1)\rightarrow(-\frac{1}{2}, 0)$ transition, then the amplitude of the two nuclear resonance signals would be equal. On the other hand, if there were complete saturation of the $(\frac{1}{2},0)\rightarrow(-\frac{1}{2}, 1)$ transition, neither of the two nuclear transitions would be seen. For Sb^{122} the forbidden lines are separated by 23 gauss from the $(\frac{1}{2},0)\rightarrow(-\frac{1}{2}, 0)$ transition. Since the full width at half-maximum of the electron lines is 3 to 5 gauss, it is unlikely that any other transition than the $(\frac{1}{2},0)\rightarrow(-\frac{1}{2}, 0)$ was saturated. The second explanation requires the introduction of relaxation processes other than the isotropic hyperfine relaxation. It is not clear just how to explain the precise form of the observed signals and the fact that the minimum counting rate occurs at approximately the same frequency for both directions of transit.

The following method of analysis was used to calculate the hyperfine splitting and gyromagnetic ratio of the Sb^{122} from the observed frequencies. If the frequency in Mc/sec of the $(-\frac{1}{2}, -1)\rightarrow(-\frac{1}{2}, 0)$ transition is denoted by ν_1 and the frequency of the $(-\frac{1}{2}, 1)\rightarrow(-\frac{1}{2}, 0)$ transition by ν_2, then from Eq. (11) the following expression can be obtained for the sum of $\nu_1+\nu_2$:

$$\nu_1+\nu_2=A_{122}'+2g_{122}'\left(\frac{\mu_n}{h}\right)H-\frac{(A_{122}')^2}{4(\mu_0/h)H}, \quad (33)$$

where A_{122}' is the absolute value of the hyperfine interaction constant of Sb^{122} expressed in Mc/sec, g_{122}' is the absolute value of the gyromagnetic ratio of Sb^{122}, and μ_0/h and μ_n/h are expressed in Mc/sec gauss. Eisinger and Feher[18] have measured very precisely the hyperfine constants of the stable Sb^{121} and Sb^{123} in a doped silicon crystal. They find

$$\begin{aligned} A_{121}&=186.802\pm0.005 \text{ Mc/sec},\\ A_{123}&=101.516\pm0.004 \text{ Mc/sec}. \end{aligned} \quad (34)$$

TABLE III. Measured values of the nuclear transition frequencies. The magnetic field is in gauss and the frequencies in Mc/sec. ν_1 corresponds to the $(-\frac{1}{2}, -1)\rightarrow(-\frac{1}{2}, 0)$ transition and ν_2 to the $(-\frac{1}{2}, 1)\rightarrow(-\frac{1}{2}, 0)$ transition. The up and down refer to whether the measurement was made with the low-frequency oscillator increasing or decreasing in frequency.

Magnetic field	Going up ν_1	Going down ν_2
8324	...	72.33±0.20
8306	71.81±0.20	...
8314	71.80±0.15	72.34±0.15
8483	71.96±0.10	72.58±0.10
8477	72.07±0.10	72.63±0.10
8475	71.91±0.10	72.60±0.10

They have also remeasured[19,20] the nuclear gyromagnetic ratio of the stable isotopes and computed the hyperfine anomaly. The values obtained are

$$\begin{aligned} &g_{121}=1.3440\pm0.0006,\\ &g_{123}=0.7281\pm0.0003,\\ &\Delta=\left(\frac{A_{121}}{A_{123}}\right)\left(\frac{g_{123}}{g_{121}}\right)-1=-(0.352\pm0.005)\%. \end{aligned} \quad (35)$$

For calculations in this paper the hyperfine anomaly will be assumed to be zero and the simple Fermi-Segrè formula[21] used to compute the gyromagnetic ratio of Sb^{122}. In terms of Sb^{121},

$$g_{122}=g_{121}A_{122}/A_{121}; \quad (36)$$

in terms of Sb^{123},

$$g_{122}=g_{123}A_{122}/A_{123}. \quad (37)$$

[18] J. Eisinger and G. Feher, Phys. Rev. **109**, 1172 (1956).
[19] W. G. Proctor and F. C. Yu, Phys. Rev. **81**, 20 (1951).
[20] Cohen, Knight, Wentink, and Koski, Phys. Rev. **79**, 191 (1950).
[21] E. Fermi and E. G. Segrè, Z. Physik **82**, 729 (1933).

If Eqs. (36) and (37) are now used to eliminate g_{122} in Eq. (33), two equations can be obtained for A_{122}' in terms of the observed frequencies. By use of these equations and the data in Table III, the following mean values are obtained for the hyperfine interaction constant and the nuclear gyromagnetic ratio of Sb^{122}. From Eq. (36),

$$\begin{aligned} |A_{122}|&=132.57\pm0.1 \text{ Mc/sec},\\ |g_{122}|&=0.954\pm0.001; \end{aligned} \quad (38)$$

from Eq. (37),

$$\begin{aligned} |A_{122}|&=132.61\pm0.1 \text{ Mc/sec},\\ |g_{122}|&=0.951\pm0.001. \end{aligned} \quad (39)$$

To obtain the final values for the radioactive Sb^{122}, an average is taken and an upper limit of 1% is assumed for the Sb^{121}/Sb^{122} and the Sb^{123}/Sb^{122} hyperfine anomalies. The final values are

$$\begin{aligned} A_{122}&=-132.59\pm0.1 \text{ Mc/sec},\\ g_{122}&=-0.952\pm0.010. \end{aligned} \quad (40)$$

C. Determination of the Nuclear Spin

In order to verify the spin 2 which has been assigned to Sb^{122} from a study of the systematics of nuclear decay schemes, a search was made for other forbidden transitions. Since the change in the σ-position counting rate is expected to be small for the $(\frac{1}{2}, -2)\rightarrow(-\frac{1}{2}, -1)$ transition, a second counter was added so that the counting rate in the σ and π positions could be observed simultaneously. These observations were made by moving the magnetic field to the proper position with the radio-frequency power turned off and then observing the change in counting rate when the radio-frequency power was turned on. Figure 12 shows the counting rate in the σ and π positions when the $(\frac{1}{2}, -1)\rightarrow(-\frac{1}{2}, 0)$ transition is saturated; Fig. 13 shows the counting rate

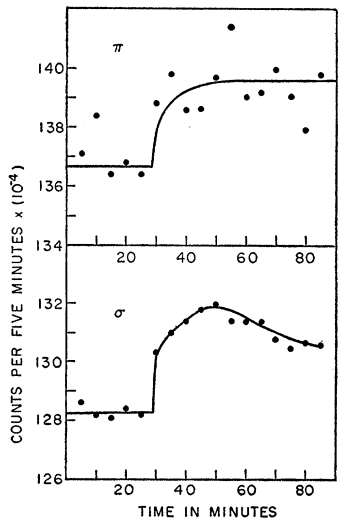

FIG. 12. Plot of counting rate *versus* time for both σ and π positions and saturation of the $(\frac{1}{2}, -1)\rightarrow(-\frac{1}{2}, 0)$ transition.

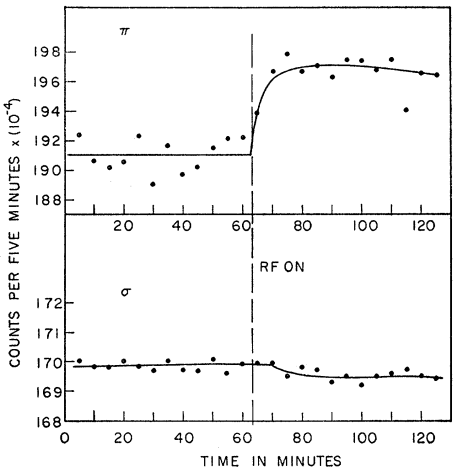

FIG. 13. Plot of counting rate *versus* time for both σ and π position and for saturation of the $(\frac{1}{2},1)\rightarrow(-\frac{1}{2},2)$ transition.

when the $(\frac{1}{2},1)\rightarrow(-\frac{1}{2},2)$ transition is saturated. No other transitions were found. The difference in stability of the π and σ counters is a graphic demonstration of the value of the feedback circuit which keeps the Sb^{122} photopeak at a constant voltage.

CONCLUSIONS

The nuclear magnetic moment of Sb^{122} has been found to be

$$\mu_{122}=(-1.904\pm0.020)\mu_n.$$

The usual odd proton—odd neutron shell-model configuration assigned to Sb^{122} is $g_{7/2}-h_{11/2}$. The simple j–j coupling shell model can be used to calculate the magnetic moment[22] of Sb^{122} from the empirical moments of the $g_{7/2}$ proton and the $h_{11/2}$ neutron. For the $g_{7/2}$ proton the neighboring nucleus Sb^{123} can be used:

$$g(g_{7/2})=0.728.$$

No element with an odd $h_{11/2}$ neutron has been measured. However, an empirical extrapolation, on the basis that the magnetic moment of an $h_{11/2}$ neutron will deviate from the Schmidt lines by as much as a $g_{9/2}$ neutron, gives the value

$$g(h_{11/2})=-0.182.$$

Using these empirical values, the expression

$$\mu_{122}(\text{theo})=-2.46$$

is obtained for the Sb^{122} nuclear magnetic moment. The agreement with the experimental value is fair.

The orientation signals indicate that the nuclear relaxation time is much shorter for the radioactive antimony donors than for the radioactive arsenic donors.[7] Part of the difference might be attributed to the fact that the concentration of Sb^{122} is approximately ten times that of As^{76}; part of it might be attributed to a difference in the magnitude of the quadrupole moments of the two nuclei. The annealing procedure for the two experiments was the same but it is still difficult to rule out completely radiation damage. One very significant difference is that it is quite easy to orient the Sb^{122} by the Overhauser method, while all such experiments on the As^{76} failed. The Sb^{122} experiments seem to imply the necessity for some nuclear relaxation mechanism in addition to that produced by modulation of the isotropic hyperfine interaction.

Preliminary experiments indicate that the relative contribution of the various angular momenta to the beta decay is approximately the same in Sb^{122} as in As^{76}.[6] The shorter nuclear relaxation time complicates this analysis.

ACKNOWLEDGMENTS

The author is particularly indebted to Dr. Walter Brown and the Bell Telephone Laboratories for the gift and cutting of the doped silicon sample. He is also indebted to Professor R. V. Pound for informing him of the suggestion by Dr. A. Abragam that a time-dependent anisotropic hyperfine interaction would furnish an additional relaxation mechanism. Thanks are expressed to Mr., Glen A. Rebka for numerous discussions and a critical reading of the manuscript.

[22] R. J. Blin-Stoyle, Revs. Modern Phys. **28**, 92 (1956).